Mechanisms of N-Demethylations Catalyzed by High-Valent Species of Heme Enzymes: Novel Use of Isotope Effects and Direct Observation of Intermediates

ARTICLE *in* JOURNAL OF THE AMERICAN CHEMICAL SOCIETY · SEPTEMBER 1998

Impact Factor: 12.11 · DOI: 10.1021/ja981357u

5 AUTHORS, INCLUDING:

Yoshihito Watanabe
Nagoya University
231 PUBLICATIONS **7,329** CITATIONS
SEE PROFILE

Jeffrey P Jones
Washington State University
111 PUBLICATIONS **3,347** CITATIONS
SEE PROFILE

Mechanisms of N-Demethylations Catalyzed by High-Valent Species of Heme Enzymes: Novel Use of Isotope Effects and Direct Observation of Intermediates

Yoshio Goto,[†] Yoshihito Watanabe,*[,†,‡] Shunichi Fukuzumi,[§] Jeffrey P. Jones,[∥] and Joseph P. Dinnocenzo[⊥]

Department of Structural Molecular Science
The Graduate University for Advanced Studies
Myodaiji, Okazaki, 444-8585 Japan
Institute for Molecular Science
Myodaiji, Okazaki 444-8585 Japan
Department of Applied Chemistry
Osaka University, Suita, 565 Japan
Departments of Pharmacology and Chemistry
University of Rochester, Rochester, New York 14642

Received April 21, 1998

The molecular mechanisms of amine N-demethylation by heme enzymes including peroxidases and cytochrome P450 have been studied for over three decades.[1−14] While the overall reaction mechanism consists of α-hydroxylamine formation followed by hydrolysis to afford N-demethylated products and formaldehyde, the mechanism of α-hydroxylamine formation is still controversial. Large intramolecular isotope effects observed for the N-demethylation of *N*,*N*-dimethylaniline (DMA)[3,5,6,13,14] have been interpreted to be due either to direct hydrogen abstraction or to proton transfer from the aminium radical, which is the one-electron oxidation product of the amine. In the case of horseradish peroxidase (HRP)-catalyzed oxidation of several amines, the corresponding aminium radicals have been detected by EPR to support the involvement of the electron-transfer process before the α-hydroxylation (Scheme 1).[8,9] On the other hand, the mechanism of the N-demethylation catalyzed by P450 is still under debate.[3,5,13] It has recently been disclosed that the magnitude of the intramolecular isotope effects on P450-catalyzed N-demethylations of substituted DMAs determined by product analysis are nearly identical to those on H-atom abstraction by a *tert*-butoxyl radical (^{t}BuO$^\bullet$).[13,14] This result suggests the involvement of H-atom abstraction in the P450 reaction. However, direct observation of the oxidation process is crucial for elucidation of the detailed mechanism.

Scheme 1

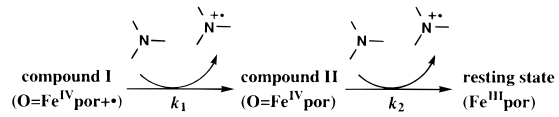

We have examined the N-demethylation mechanisms through novel isotope effect studies carried out by direct observation of the reduction of the high-valent species responsible for catalysis. Reactions of compound I of HRP and of O═Fe^{IV}TMP porphyrin π-cation radical (which serves as a functional model for the active species of cytochrome P450) with a series of para-substituted dimethylanilines (DMAs) have been investigated (TMP = 5,10,15,20-tetramesitylporphine dianion). The dependence of the rate constants on the one-electron oxidation potentials of DMAs and the comparison of the *kinetic* and *product* isotope effects have allowed us to clarify the mechanism of N-demethylation.

Upon the mixing of HRP compound I and DMAs under stopped-flow conditions in a buffer solution (pH 7.0) at 273K,[15] rapid formation of compound II (k_1) and the following relatively slow conversion (k_2) to the resting state were observed. The same reactions were also carried out with deuterated compounds (DMAs(-CD_3)$_2$)[16] to determine k_{1D} and k_{2D}. The k_1 and k_2 values and the KIEs (k_{1H}/k_{1D} and k_{2H}/k_{2D}) are listed in Table 1 together with the one-electron oxidation potentials (E^0) of DMAs.[17] Both the k_1 and k_2 values increase with decrease in the E^0 value. A linear correlation between log k_1 and E^0 is shown in Figure 1a.[18] No kinetic isotope effects (KIEs) are observed for either k_1 or k_2. The dependence of k_1 and k_2 on E^0 and the absence of KIEs clearly indicate that the rate-determining steps are the electron transfers from DMA to HRP compound I and compound II, respectively.

While transient formation of compound I of P450 has been reported, because it is formed in a mixture of other species,[19] it has not been fully characterized. Thus, we have employed O═Fe^{IV}TMP$^{\bullet+}$ (**1**)[20] as a model complex for the proposed high-valent catalytic intermediate of P450 in the kinetic measurement of N-demethylation of DMAs since **1** is able to mimic most P450-catalyzed oxidations. The reactions of **1** with DMAs in CH_2Cl_2 at 223 K were monitored by UV−vis spectral changes of **1** and found to afford Fe^{III}TMP without observation of any intermediates.[21] The rate constants (k_3) and *kinetic isotope effects* (k_{3H}/k_{3D}) are summarized in Table 1. In addition, *product (intramolecular) isotope effects* (k_H/k_D)[22] are observed in the reactions of **1** with DMAs(-CD_3, -CH_3)[16] as listed in Table 1.

Figure 1b shows a linear correlation between log k_3 and E^0 similar to the correlation observed for log k_1 and E^0 (Figure 1a).

[†] The Graduate University for Advanced Studies.
[‡] Institute for Molecular Science.
[§] Osaka University.
[∥] Department of Pharmacology, University of Rochester.
[⊥] Department of Chemistry, University of Rochester.

(1) Ortiz de Montellano, P. R. *Cytochrome P450. Structure, Mechanism, and Biochemistry*, 2nd ed.; Plenum Publishing Corporation: New York, 1995.
(2) Guengerich, F. P.; Macdonald, T. L. *Acc. Chem. Res.* **1984**, *17*, 9−16.
(3) Miwa, G. T.; Walsh, J. S.; Kedderis, G. L.; Hollenberg, P. F. *J. Biol. Chem.* **1983**, *258*, 14445−14449.
(4) Miwa, G. T.; Garland, W. A.; Hodshon, B. J.; Lu, A. Y. H.; Northrop, D. B. *J. Biol. Chem.* **1980**, *255*, 6049−6054.
(5) Guengerich, F. P.; Yun, C.-H.; Macdonald, T. L. *J. Biol. Chem.* **1996**, *271*, 27321−27329.
(6) Okazaki, O.; Guengerich, F. P. *J. Biol. Chem.* **1993**, *268*, 1546−1552.
(7) Macdonald, T. L.; Gutheim, W. G.; Martin, R. B.; Guengerich, F. P. *Biochemistry* **1989**, *28*, 2071−2077.
(8) Griffin, B. W.; Ting, P. L. *Biochemistry* **1978**, *17*, 2206−2211.
(9) Van der Zee, J.; Duling, D. R.; Mason, R. P.; Eling, T. E. *J. Biol. Chem.* **1989**, *264*, 19828−19836.
(10) Kedderis, G. L.; Hollenberg, P. F. *J. Biol. Chem.* **1983**, *258*, 8129−8138.
(11) Kedderis, G. L.; Koop, D. R.; Hollenberg, P. F. *J. Biol. Chem.* **1980**, *255*, 10174−10182.
(12) Lindsey Smith, J. R.; Mortimer, D. N. *J. Chem. Soc., Perkin Trans. 2* **1986**, 1743−1749.
(13) Manchester, J. I.; Dinnocenzo, J. P.; Higgins, L.; Jones, J. P. *J. Am. Chem. Soc.* **1997**, *119*, 5069−5070.
(14) Karki, S. B.; Dinnocenzo, J. P.; Jones, J. P.; Korzekwa, K. R. *J. Am. Chem. Soc.* **1995**, *117*, 3657−3664.

(15) Kinetic experiments involving HRP compounds I and II were performed with a Hi-Tech SF-43 stopped-flow instrument. Compound I was prepared by mixing with a stoichiometric amount of H_2O_2 followed by mixing with 10−100 equiv of DMA at 273 K in 50 mM phosphate buffer (pH 7.0) with double-mixing mode (delay time, 10 ms; final concentration of HRP, 2.5 μM). The UV−vis spectral changes showed rapid conversion of compound I to compound II (Supporting Information). The rate of compound II formation (k_1) was determined by fitting the change in absorbance at 411 nm with a least-squares procedure; the fit was linearly dependent on the concentration of the substrates. Compound II was prepared by addition of stoichiometric amounts of H_2O_2 to a solution of ferric HRP followed by reduction with stoichiometric amounts of potassium ferricyanide. The reaction rate (k_2) of compound II and DMA was also determined from the absorbance change at 403 nm by a similar method.

(16) Dinnocenzo, J. P.; Karki, S. B.; Jones, J. P. *J. Am. Chem. Soc.* **1993**, *115*, 7111−7116.

(17) Oxidation potentials of DMAs were determined by cyclic voltammetric measurements (BAS 100B/W) in CH_2Cl_2 containing 2 mM DMA derivatives and 50 mM tetrabutylammonium hexafluorophosphate at 223 K with a voltage sweep rate of 100−200 mV/s.

(18) The linear correlation between log k_2 and E^0 was also observed.

(19) Egawa, T.; Shimada, H.; Ishimura, Y. *Biochem. Biophys. Res. Commun.* **1994**, *201*, 1464−1469.
(20) Groves, J. T.; Watanabe, Y. *J. Am. Chem. Soc.* **1988**, *110*, 8443−8452.

10.1021/ja981357u CCC: $15.00
Published on Web 10/01/1998

Table 1. Bimolecular Rate Constants and the Isotope Effects of the Reactions of HRP Compounds I, II and O═Fe^{IV}TMP$^{\bullet+}$ with a Series of Para-substituted DMAs of which Oxidation Potentials Are in the Second Column from the Left

para-substituent of DMA	E^0 [V vs Fc]	HRP system				TMPFe system		
		k_1[b] [M^{-1} s^{-1}]	k_{1H}/k_{1D}	k_2[b] [M^{-1} s^{-1}]	k_{2H}/k_{2D}	k_3[b] [M^{-1} s^{-1}]	k_{3H}/k_{3D}	k_H/k_D
OMe	0.14	$(9.5 \pm 0.6) \times 10^7$	1.0 ± 0.1	$(4.6 \pm 0.1) \times 10^6$	1.0 ± 0.1	$(5.6 \pm 0.1) \times 10^7$	1.3 ± 0.1	3.9 ± 0.1
Me	0.33	$(3.1 \pm 0.1) \times 10^7$	1.0 ± 0.1	$(2.1 \pm 0.1) \times 10^5$	1.0 ± 0.1	$(2.7 \pm 0.1) \times 10^5$	1.5 ± 0.1	3.8 ± 0.1
H	0.53[a]	$(6.0 \pm 0.3) \times 10^5$	1.1 ± 0.1	$(1.6 \pm 0.1) \times 10^4$	1.1 ± 0.1	$(1.7 \pm 0.1) \times 10^4$	1.9 ± 0.2	2.8 ± 0.1
Cl	0.49	$(1.6 \pm 0.1) \times 10^6$	1.0 ± 0.1	$(3.2 \pm 0.2) \times 10^4$	1.0 ± 0.1	$(3.4 \pm 0.1) \times 10^3$	1.8 ± 0.1	2.6 ± 0.1
Br	0.47	$(1.8 \pm 0.1) \times 10^6$	1.0 ± 0.1	$(3.4 \pm 0.2) \times 10^4$	1.0 ± 0.1	$(6.6 \pm 0.1) \times 10^3$	2.0 ± 0.1	3.4 ± 0.1
CN	0.82	$(8.7 \pm 0.8) \times 10^2$	1.0 ± 0.2	nd[c]	nd	$(9.0 \pm 0.4) \times 10$	5.5 ± 0.4	6.9 ± 0.1
NO_2	0.92	nd	nd	nd	nd	$(2.2 \pm 0.1) \times 10$	5.9 ± 0.4	6.2 ± 0.9

[a] Peak potential was used because no reversible wave was detected on cyclic voltammetry. [b] Determined by the experiments with DMA derivatives of which methyl groups are not deuterated. [c] Not determined.

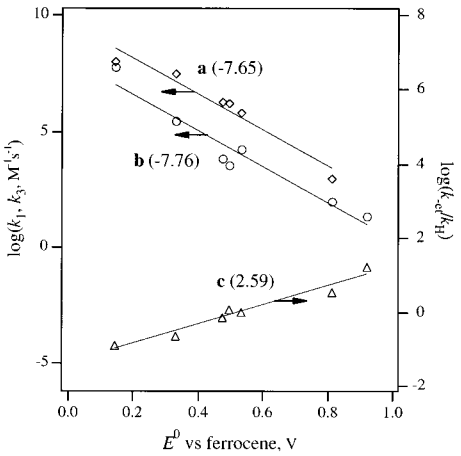

Figure 1. Dependence of kinetic values on the oxidation potential of DMAs (E^0). The slopes of each line are shown in parentheses. (a) (diamond): bimolecular rate constant of HRP compound I with DMAs, k_1. (b) (circle): bimolecular rate constant of O═Fe^{IV}TMP$^{\bullet+}$ with DMAs, k_3. (c) (triangle): k_{-et}/k_H determined by eq 2.

The parallel relationship between these two plots indicates that electron transfer from the DMAs is similar for HRP and the model complex. However, the KIEs are observed only for the reactions of O═Fe^{IV}TMP$^{\bullet+}$. The k_{3H}/k_{3D} value increases with an increase in the E^0 value to reach a value of 5.9 ± 0.4 in the case of the *p*-nitro derivative. More importantly, there is a significant difference between the *kinetic* (k_{3H}/k_{3D}) and *product* (k_H/k_D) isotope effects. Coupled with the fact that no compound II is seen as an intermediate, these isotope effects suggest that there is a significant reverse electron transfer, so that any compound II−aminium radical pair formed can partition either toward products (k_H) or to initial reactants (k_{-et}) as shown in Scheme 2. The redox potential of the DMA is likely to have a significant effect on k_{-et}. Using a steady-state assumption (the compound II−radical pair is "constant" and at a low concentration), one can derive an expression (eq 1) that relates the KIEs (k_{3H}/k_{3D}) and the product isotope effects (k_H/k_D). The product isotope effects reflect the H-atom transfer step from DMA$^{\bullet+}$ to O═Fe^{IV}TMP.

Scheme 2

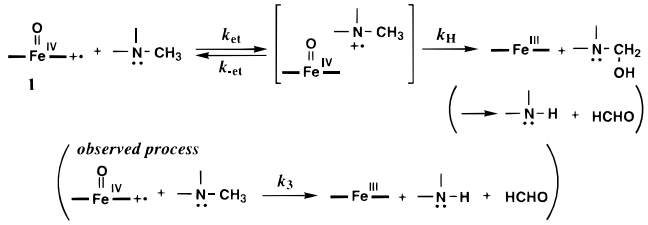

$$k_{3H}/k_{3D} = (k_H/k_D)\{(k_D/k_H) + (k_{-et}/k_H)\}/\{1 + (k_{-et}/k_H)\} \quad (1)$$

When electron transfer is the primary rate-determining step ($k_{-et}/k_H \ll 1$), eq 1 reduces to $k_{3H}/k_{3D} = 1$. On the other hand, when $k_{-et}/k_H \gg 1$, eq 1 reduces to $k_{3H}/k_{3D} = k_H/k_D$. Thus, the difference between k_H/k_D and k_{3H}/k_{3D} should decrease with an increase in k_{-et}/k_H. The k_{-et}/k_H value can be obtained from the k_{3H}/k_{3D} and k_H/k_D values using eq 2, which is derived from eq 1.

$$k_{-et}/k_H = \{(k_{3H}/k_{3D}) - 1\}/\{(k_H/k_D) - (k_{3H}/k_{3D})\} \quad (2)$$

The k_{-et} value for the back electron transfer from O═Fe^{IV}TMP to DMA$^{\bullet+}$ is expected to increase with an increase in E^0 , the one-electron reduction potential of DMA$^{\bullet+}$. On the other hand, the H-atom transfer rate constant (k_H) may be less sensitive to E^0 than the back electron-transfer rate constant (k_{-et}).[23] Thus, the k_{-et}/k_H value may increase with an increase in the E^0 value. In fact, such a correlation between k_{-et}/k_H and E^0 is demonstrated in Figure 1c.

In conclusion, our results are in agreement with the currently accepted mechanism in which the N-demethylation of DMAs by HRP compounds I and II both proceed via a rate-determining electron-transfer step. Our results suggest that demethylation by O═Fe^{IV}TMP$^{\bullet+}$ also proceeds via electron transfer; however, H-atom transfer from DMAs$^{\bullet+}$ to O═Fe^{IV}TMP competes with back electron transfer, and this competition is responsible for the observed deuterium isotope effects. The difference between the *kinetic* and *product* isotope effects depends on the ratio of the rate constant of the back electron transfer to that of the hydrogen transfer.

Acknowledgment. This work was partly supported by JSPS-NSF Joint Program, Photo-Induced Charge Transfer, and also supported by a Grant-in-Aid for Priority Area, Molecular Biometallics to Y.W. from the Ministry of Education, Science, Sport, and Culture in Japan.

Supporting Information Available: UV−vis spectral changes for the reactions of DMAs with both HRP compound I and O═Fe^{IV}TMP$^{\bullet+}$, derivation of eq 1 (4 pages, print/PDF). See any current masthead page for ordering information and Web access instructions.

JA981357U

(21) Kinetic experiments on the iron−TMP complex were performed with a Hi-Tec SF-43 sequential-mixing stopped-flow instrument. In a typical run, a CH_2Cl_2 solution of Fe^{III}TMP(OH) (40 μM) was mixed with an equal volume of CH_2Cl_2 containing 4 equiv of *m*CPBA and 1 equiv of 3-chlorobenzoic acid at 223 K. Formation of **1** was complete in 3 min and confirmed by its UV−vis spectrum. DMA (10−100 equiv) in CH_2Cl_2 was then mixed with **1** (final concentration of **1**, 10 μM), a very rapid isosbestic change of **1** to Fe^{III}-TMP was observed (Supporting Information). The reaction rate constant (k_3) was determined from analysis of the change in absorbance at 413 nm.

(22) KIEs by product analysis were determined by GC-MS analyses of single turnover reactions. A 1.0 mM solution of Fe^{III}TMP(OH) was added to a CH_2Cl_2 solution containing 1.2 equiv of *m*CPBA at 223 K. After confirmation of O═Fe^{IV}TMP$^{+\bullet}$ formation, a CH_2Cl_2 solution of 10 equiv of a DMA(-CH_3, -CD_3) derivative was added. After the solution color changed to brown, trifluoroacetic anhydride was added, and the *N*-methylaniline derivative was detected as a trifluoroacetylamide form. The k_H/k_D value was determined with GC/SIM from the M^+ peak area ratio of trideuteriomethyl- and methyl-trifluoroacetylaniline (ref 16).

(23) The energetics of hydrogen transfer consist of those for transfer of a proton and for an electron. The substitution effects on the proton- and electron-transfer processes may be largely canceled out since the acidity of DMA$^{\bullet+}$ increases but the donor ability of DMA(-H)$^{\bullet}$ decreases with an increase E^0.